Respective Contributions of Polar vs Enthalpy Effects in the Addition/Fragmentation of Mercaptobenzoxazole-Derived Thiyl Radicals and Analogues to Double Bonds

J. Lalevée,* X. Allonas, F. Morlet-Savary, and J. P. Fouassier

Department of Photochemistry, UMR 7525 CNRS, University of haute Alsace, ENSCMu, 3 rue Alfred Werner, 68093 Mulhouse Cedex France

Received: May 16, 2006; In Final Form: August 23, 2006

The formation and the reactivity of three selected sulfur-centered radicals formed from mercaptobenzoxazole, mercaptobenzimidazole, and mercaptobenzothiazole toward four double bonds (methyl acrylate, acrylonitrile, vinyl ether, and vinyl acetate) are investigated. The reversibility of the addition/fragmentation reaction in these widely used photoinitiating systems of radical polymerization was studied, for the first time, through the measurement of the corresponding rate constants by time-resolved laser spectroscopy. The combination of these results with quantum mechanical calculations clearly evidences that, contrary to previous studies on other aryl thiyl radicals, the addition rate constants (k_a) are governed here by the polar effects associated with the very high electrophilic character of these radicals. However, interestingly, the back-fragmentation reaction (k_{-a}) is mainly influenced by the enthalpy effects as supported by the relationship between the rate constants and the addition reaction enthalpy ΔH_R. The addition and fragmentation rate constants calculated from the transition state theory (TST) are in satisfactory agreement with the experimental ones. Therefore, molecular orbital (MO) calculations offered new opportunities for a better understanding of the sulfur-centered radical reactivity.

Introduction

The different factors affecting the reactivity of radicals toward the addition reaction to a double bond remain the subject of fascinating discussions in the literature.[1−10] This elementary process is particularly important for single bond formation and plays a key role in chemistry; for example, in polymerization reactions.[11] Mercaptans such as mercaptobenzoxazole (MBO), mercaptobenzimidazole (MBI) and mercaptobenzothiazole (MBT) are used as co-initiators of polymerization, e.g., in thiol-ene chemistry (where the classical ketone/mercaptan photoinitiating system leads to photoreduction and generates sulfur-centered radicals) or in direct laser imaging applications (where the bisimidazole derivatives (HABI)/mercaptan system allows us to generate also these radicals through a hydrogen transfer from a thiol derivative to the lophyl radical formed upon the photolysis of HABI).[11a] However, the addition properties of these radicals to a monomer double bond M and the further back-fragmentation reaction of the adduct radical remain both largely unknown. The knowledge of the processes is obviously important for getting a high efficiency of the polymerization initiation step.

The reactivity of sulfur-centered radicals has clearly deserved much less attention than that of carbon-centered structures.[1−2,12−14] Despite many efforts mostly devoted to aryl thiyl radicals,[12−15] different important questions on this reactivity still remain. Experimental data on sulfur-centered radicals are rather scarce. Recently, the importance of polar effects has been examined through molecular orbital calculations for the hydrogen-atom-transfer reaction of the model thiyl radicals.[16] The relative contribution of the polar and enthalpy effects and the factors that govern the addition/fragmentation process are outstanding problems.

The addition reaction of a radical to a double bond (DB) is usually depicted by a state correlation diagram (SCD),[1,5−8] which shows the potential energy profiles of the four lowest doublet configurations of the system consisting of the radical unpaired electron and the attacked π bond electron pair: the reactant ground state, the reactant excited state and two charge-transfer configurations (CTC) R^+/DB^- and R^-/DB^+. According to this diagram, the barrier obviously decreases upon increasing exothermicity. Moreover, the involvement of the polar effects can also greatly influence the reaction through a decrease of the barrier when the CTC energies decrease.[1,7,8,17−28] This has been recently exemplified in the study of the reactivity of a large class of carbon-centered radicals toward different alkenes:[25−28] A clear separation and a quantification of both polar and enthalpy factors were proposed.

In this paper, the reactivity of three selected large sulfur-centered radicals (derived from MBO, MBI, MBT) toward four alkenes usable as monomers (vinyl ethyl ether VE, vinyl acetate VA, methyl acrylate MA, acrylonitrile AN) will be investigated, for the first time, through laser flash photolysis LFP and quantum mechanical calculations. The aim of our work is 2-fold. First, it will provide a set of 20 new rate constants for the addition and fragmentation processes (these values were unknown). Second, quantum mechanical calculations will offer a good opportunity for a better understanding of the reactivity of these sulfur-centered radicals toward the addition/fragmentation and give a first insight on the key factors governing both processes. The expected strong enthalpy/polar effects (these double bonds having very different electron acceptor/donor properties) will be discussed.

* Corresponding author. E-mail: j.lalevee@uha.fr. Tel: 33 (0)389336837. Fax: 33 (0)389336895.

10.1021/jp062991u CCC: $33.50
Published on Web 09/27/2006

CHART 1

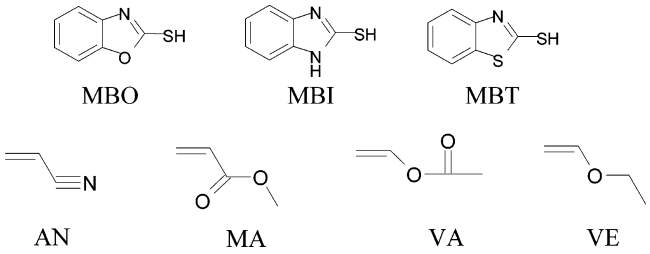

Experimental Part and Computational Procedure

The formulas of the three mercaptans (mercaptobenzoxazole MBO, mercaptobenzimidazole MBI, mercaptobenzothiazole MBT), 2,2′-dithiobis(benzothiazole) and alkenes, obtained from Aldrich, are represented in Chart 1.

All rate constants were determined by nanosecond laser flash photolysis LFP in acetonitrile. The setup, based on a pulsed Nd:Yag laser (Powerlite 9010, Continuum) operating at 10 Hz and delivering nanosecond pulses at 355 nm, has been already described in detail (resolution time: 10 ns).[11b] The experiment on the picosecond time scale used a pump−probe arrangement involving a YAG/Nd laser. This second experimental setup is characterized by a time resolution of about 10 ps and has been fully presented in ref 29. All the experiments were carried out at 298 K.

Computational Procedure

Quantum mechanical calculations have been performed with the Gaussian 03 suite of programs.[30] Reactants, products, and transition states were fully optimized at the B3LYP/6-31G* level. The addition reaction enthalpy (ΔH_R) was calculated as the energy difference between the product and the reactants at this level and was ZPE corrected. From the B3LYP/6-31G* transition state (TS) structure, the amount of charge δ^{TS} transferred from the radical to the alkene evaluated from the Mulliken charges was calculated at the 6-31G* and 6-311++G** levels. δ^{TS} will be positive for a nucleophilic radical and negative for an electrophilic one. The barrier (E_a^{TS}) was evaluated by performing UB3LYP/6-311++G** single point energies on the corresponding UB3LYP/6-31G* structures (UB3LYP/6-311++G**//UB3LYP/6-31G* level) and ZPE corrected at the UB3LYP/6-31G* level. The activation energy for the addition reaction is obtained from the enthalpy changes between the reactants and the TS structure (ΔH^*) in eq 1,[31,32]

$$E_a = \Delta H^* + (1 - \Delta n^*)RT \qquad (1)$$

where Δn^* is the number of particle changes when going to the TS structure. The thermal energy corrections in ΔH^* were calculated for $T = 298$ K.[31]

The rate constants of addition and fragmentation were also calculated: the determination of the preexponential factor in the Arrhenius equation (A) is given by the activated complex theory:[31,32]

$$A = \chi\frac{\kappa T}{h}(R'T)^{-\Delta n^*}\exp(1 - \Delta n^*)\exp\left(\frac{\Delta S^*}{R}\right) \qquad (2)$$

ΔS^* is the entropy changes in going to the TS structure, κ is the Boltzmann constant, R is the ideal gas constant, T is the temperature in absolute units, h is Planck's constant, and χ is the transmission coefficient (taken here equal to 1). The harmonic oscillator approximation was adopted for the ΔS^* calculations, allowing the determination of A by eq 2.[30] This treatment was assumed as accurate enough to describe the addition of carbon-centered radicals to double bonds.[32] From the calculated activation energy and the preexponential factor, the calculated addition/fragmentation rate constants were given by the well-known Arrhenius equation.

Adiabatic ionization potentials (IP) and adiabatic electron affinities (EA) characterizing the reactants were calculated from the energies of the relaxed neutral molecule and the corresponding relaxed ion at the B3LYP/6-31+G* level and were ZPE corrected at the same level.

The electronic absorption spectra were calculated with the time dependent density functional theory at the MPW1PW91/6-31G* level on the relaxed geometry determined at the UB3LYP/6-31G* level.

SCHEME 1

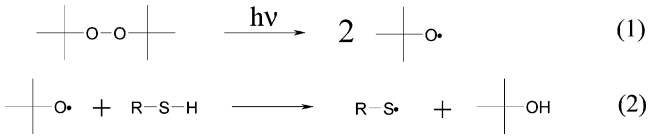

Results and Discussions

A. Generation of Sulfur-Centered Radicals. Thiyl radicals can be usually generated through three different methods:[33,34] (i) the hydrogen-transfer reaction between a thiol and a radical, (ii) photodissociation of a disulfide, and (iii) reaction of thiols with excited carbonyl compounds (usually in their triplet state). In this paper, only the first two methods were used. Indeed, the quantum yield for the thiyl radicals formation is usually low when using the third method; i.e., this approach is undesirable for an investigation of sulfur-centered radicals reactivity.[35] The mechanism involved in this last process, which is beyond the scope of the present paper, is, however, basically interesting and will be examined in detail in a forthcoming paper.

1. Hydrogen-Transfer Reaction. The sulfur radicals are efficiently produced by hydrogen-transfer reaction, as reported in Scheme 1, similar to that employed in ref 36 to produce aminoalkyl radicals. A two-step process is used: generation of a *tert*-butoxyl radical through the photochemical decomposition of *tert*-butylperoxide (1) and RS−H hydrogen abstraction reaction (2). The produced sulfur-centered radicals can be directly observed (Figure 1). For sake of clarity, in the following discussion, the radicals generated from MBO, MBI and MBT will be referred as R_1, R_2, and R_3 respectively. The rate constants of interaction

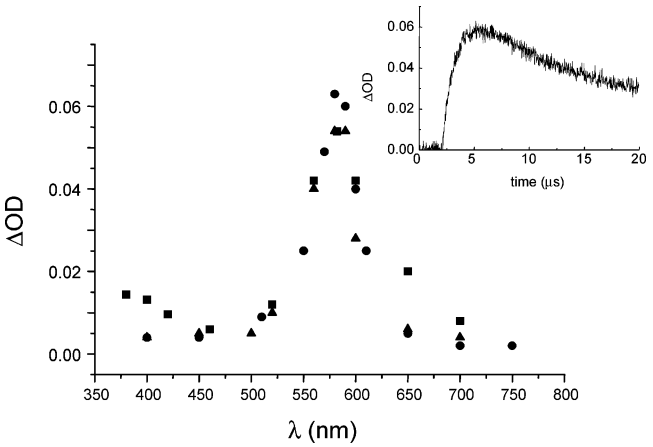

Figure 1. Transient absorption spectra observed 2 μs after the laser flash in acetonitrile: R_1 (■); R_2 (▲); R_3 (●). The quantity k_q[mercaptan] was kept constant (this corresponds to a rise time about 800 ns). Inset: kinetic corresponding to the R_2 radical formation at 580 nm.

TABLE 1: Rate Constants of Interaction between the *tert*-Butoxyl Radical and the Mercaptans[a]

	$10^{-9}k_q$ (M^{-1} s^{-1})	λ_{max}(exp)[b] (nm)	λ_{max}(calc)[c] (nm)	BDE(S−H) (kcal/mol)[d]
MBO	1.0	580	507	82.8
MBI	2.2	580	506	80.7
MBT	2.1	580	510	83.2

[a] Absorption maximum of the thiyl radicals. Bond dissociation energy of S−H. [b] Experimental values in acetonitrile. [c] Calculated values (see text). [d] Evaluated from isodesmic reaction at UB3LYP/6-31G* level and ZPE corrected.

k_q between the *tert*-butoxyl radical and the different mercaptans, determined from the rise time of the sulfur-centered radicals at 580 nm (Figure 1) through a classical Stern−Volmer approach, are gathered in Table 1. The sulfur-centered radical absorption decays according to a second-order law in the 100 μs time scale and is not affected by the presence of oxygen (the interaction rate constant is estimated to be lower than 10^6 M^{-1} s^{-1}).

The absorption spectra of these radicals (Figure 1) are characterized by the same intense absorption band centered at about 580 nm in acetonitrile. For R_3, a similar spectrum has been previously reported in ref 12. Calculations of the absorption spectra predict a very similar absorption wavelength maximum around 510 nm (Table 1). Despite a systematic deviation of about 70 nm, also observed with an extended basis set (6-311++G**) and with different functionals (B3LYP; PBE1PBE; BLYP), the electronic absorption spectra of R_1−R_3 are found to be very similar, evidencing the weak influence of the O, N, or S heteroatoms. This deviation is likely due to the TDDFT method as noted for other systems exhibiting a part of charge-transfer character in the electronic transition.[37] On the other side, calculated and experimental spectra of, e.g., acrylate radicals are in excellent agreement.[38] For MBI, only the sulfur-centered radical is experimentally observed (Figure 1) ruling out the possibility of a hydrogen abstraction from the N−H bond.

The S−H bond dissociation energy (BDE) directly governs the exothermicity of such a hydrogen-transfer reaction.[2b,39] The most accurate calculated BDEs are usually derived from the enthalpy of isodesmic reactions.[30b] In our case, this is reaction 3′. The reaction enthalpy ($\Delta H_3'$) is evaluated from DFT calculations and the BDEs are deduced from eq 3 using the recently established BDE value of 83.5 kcal/mol for Ph−S−H.[40]

$$RS{-}H + Ph{-}S^{\bullet} \rightarrow RS^{\bullet} + Ph{-}SH \qquad (3')$$

$$BDE(RS{-}H) = BDE(PhS{-}H) + \Delta H_3' \qquad (3)$$

The determined BDEs are gathered in Table 1: very similar values are obtained for MBO, MBI, and MBT. Despite a systematic error that might be ascribed to the isodesmic reaction used[41] and knowing the BDE of *tert*-butyl alcohol (105 kcal/mol),[39] the hydrogen-transfer reaction appears here as highly exothermic (reaction 2 in Scheme 1): the reaction enthalpy is close to −24 kcal/mol for the three mercaptans which accounts for the rather similar and very high rate constants observed.

2. Photodissociation of Disulfides. The photodissociation of disulfides also leads to an efficient generation of thiyl radicals:[33,34]

$$RS{-}SR \xrightarrow{h\nu} 2RS^{\bullet} \qquad (4')$$

To confirm the experimental assignment of the sulfur radical absorption, 2,2′-dithiobis(benzothiazole), which is the only commercial compound of interest in the present case, was selected as a suitable disulfide. The cleavage process of this disulfide is investigated for the first time on a picosecond time scale. After excitation at 355 nm of 2,2′-dithiobis(benzothiazole), the R_3 radical is directly generated and exhibits a spectrum identical (Figure 2) to that observed in the hydrogen-transfer experiment (Figure 1). The rise time of this species at 586 nm is found within the resolution time of our experimental setup (∼10 ps).

The two molecular orbitals (HOMO → LUMO) of 2,2′-dithiobis(benzothiazole) involved in this electronic transition are depicted in Figure 2. A $\pi \rightarrow \sigma^*$ transition is found between the HOMO delocalized π orbital and the antibonding σ^* LUMO orbital of the disulfide S−S bond. Therefore, the first excited singlet state is dissociative ($\pi\sigma^*$) toward this single bond, which quite well explains this ultrafast cleavage process.

B. Reactivity Toward Alkenes. The reactivity of R_1, R_2, and R_3 generated by the hydrogen-transfer reaction toward

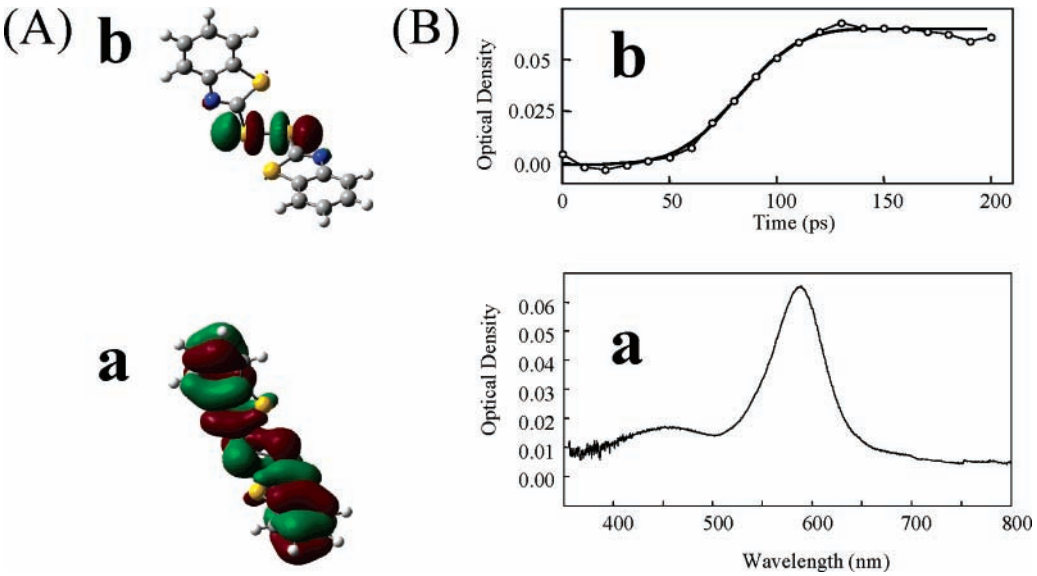

Figure 2. (A) Orbitals involved in the $\pi \rightarrow \sigma^*$ transition. (a) HOMO (orbital no. 85) and (b) LUMO (orbital no. 86) for 2,2′-dithiobis(benzothiazole). (B) Picosecond study of the photodissociation of 2,2′-dithiobis(benzothiazole) in benzene. (a) Absorption spectrum of R_3 taken 150 ps after the laser excitation. (b) Absorption of R_3 vs time at 586 nm. The fit of this trace leads to a rise time within the time resolution of the experimental setup (see text).

SCHEME 2

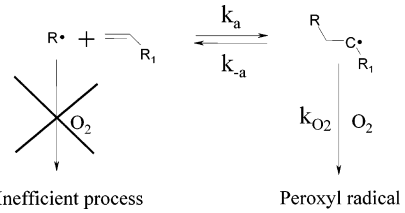

alkenes was investigated, keeping in mind that generating R_3 through photodissociation has obviously led to similar results.

1. Rate Constants of the Processes. The reversibility is one of the most characteristic feature of the addition reaction of sulfur-centered radicals to alkenes.[12−15,33−34] To determine the corresponding rate constants, we used the selective radical trapping flash photolysis method already developed [12−15] which is based on the fact that oxygen acts as a selective scavenger of the carbon-centered radical. As O_2 is not reactive toward the sulfur-centered radicals, the equilibrium established in the addition process (Scheme 2) shifts to the peroxyl side in the presence of oxygen (Figure 3).

From this scheme, the decay of R can be expressed[12] as in eq 4. When the alkene concentration increases, the recombination reaction (k_r) of the sulfur-centered radical will be neglected in the following treatment. Assuming a quasi-steady-state concentration in carbon-centered radicals $R-CH_2-C\cdot HR_1$, eq 5 holds true (k_{app} is the apparent rate constant for the disappearance of the sulfur-centered radical in the presence of alkene when $[O_2]$ is fixed).

$$-\mathrm{d}[R]/\mathrm{d}t = k_r[R]^2 + k_a[R][\text{alkene}] - k_{-a}[R-CH_2-C^{\bullet}HR_1] \quad (4)$$

$$1/k_{app} = 1/k_a + k_{-a}/(k_a k_{O_2}[O_2]) \quad (5)$$

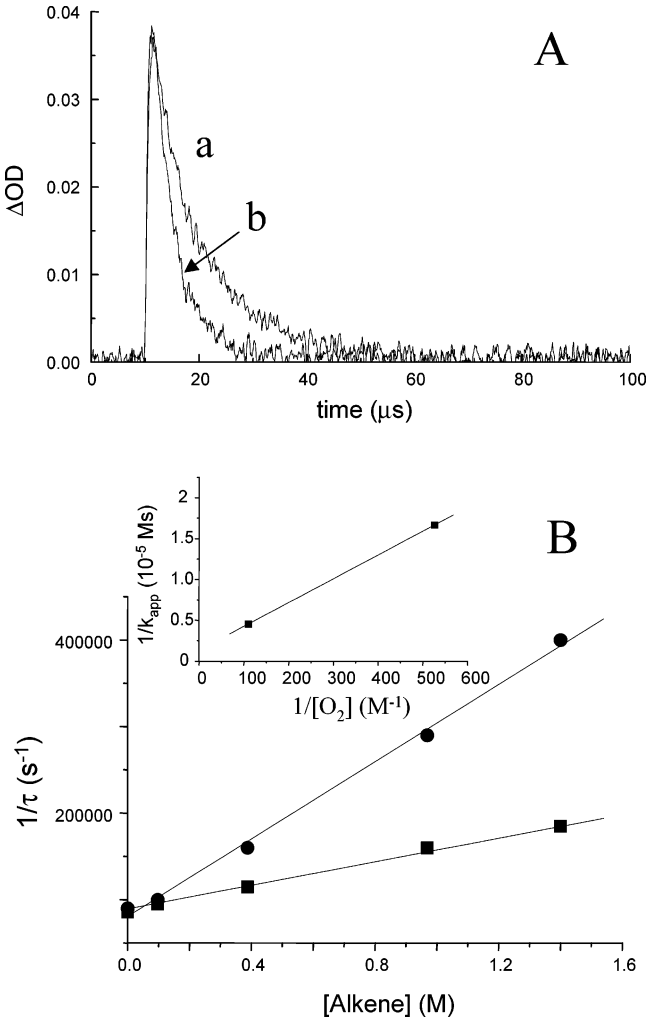

Figure 3. (A) Effect of the oxygen concentration on the decay trace at 580 nm corresponding to the R_3/VA addition reaction in acetonitrile ([VA] = 0.65 M): curve (a) nondegassed acetonitrile and curve (b) oxygen saturated acetonitrile. (B) Stern−Volmer analysis (see text) for the determination of k_{app} for the system R_3/VA in nondegassed acetonitrile (square) and in oxygen saturated acetonitrile (circle). Inset: evolution of $1/k_{app}$ with $1/[O_2]$.

At a given O_2 concentration, in aerated acetonitrile ($[O_2] = 1.9 \times 10^{-3}$ M) and in O_2 saturated acetonitrile ($[O_2] = 9.1 \times 10^{-3}$ M), a Stern−Volmer plot of the reciprocal value of the R lifetime as a function of the alkene concentration yields k_{app} (Figure 3). From eq 5, a plot of $1/k_{app}$ against $1/[O_2]$ gives a direct access to k_a and $k_{-a}/(k_a k_{O_2})$ (Figure 3). By using the k_{O_2} value (3×10^9 M^{-1} s^{-1}) recently determined for acrylate radicals,[38] both the equilibrium constant ($K = k_a/k_{-a}$) and k_{-a} can be experimentally evaluated. The kinetic analysis leading to eqs 4 and 5 is based on a steady-state assumption with respect to the concentration of the carbon-centered radicals. It has been shown that this approach can be applied to LFP experiments.[14] All the parameters obtained for the addition of R_1, R_2, and R_3 to the different alkenes are gathered in Table 2. The efficiency of the addition reaction (k_a) is strongly affected by both the radical ($R_3 > R_1 \gg R_2$) and the alkene structures (VE > VA > MA > AN). The R_3 and R_1 addition reactions are found reversible; the R_2 radical is almost nonreactive and the reversibility cannot be obviously investigated. Assuming a similar k_{O_2} value for the different alkenes (as already stated in refs 12−15), it appears that the fragmentation rate constants decrease in the order VA > VE > MA > AN. The equilibrium constants follow the opposite order (decrease from AN to VA).

2. Molecular Orbital (MO) Calculations. (a) Description of the Addition Reaction. Previous studies in the literature[1,7,8,42−46] have shown that a reliable description of the barrier for a chemical reaction is not straightforward. The ability of different computational methods for radical addition reactions has been evaluated: high-level theoretical procedures such as UQCISD-(T), CCSD(T), CBS−RAD, CBS-QB3, G2 and G3 methods were found to give excellent barrier values close to the experimental ones.[30] For an absolute description of the experimental results, the use of a very high level of theory is indubitably required. Among these procedures, the best one is certainly the G3(MP2)-RAD method widely used by Coote et al.: it has been shown very powerful, e.g., for the addition/fragmentation reaction of small radicals in RAFT polymerization, the methyl radical addition to C═S double bond, the determination of formation heats of small open shell molecules, etc.[42−46] Unfortunately, these methods can hardly be applied on large chemical systems because of far too important computer requirements.

In contrast, procedures based on the density functional theory (particularly, the UB3LYP/6-311++G**//UB3LYP/6-31G* procedure) give satisfactory results, with acceptable calculation times, as noted in the addition reactions of carbon-centered radicals to double bonds.[25,26] Our MO study is devoted here (as in refs 25 and 26) to an interpretation of the experimental trends, and not to a proposal for absolute values, by quantum mechanical calculations. Therefore, the procedure should be adequate for a first approach of the sulfur-centered radicals reactivity more especially as the same DFT method can be used on very large systems.

TABLE 2: Experimental Parameters Characterizing the Addition Reactions to Different Alkenes

	R_1			R_2			R_3		
alkene	k_a $(M^{-1}\ s^{-1})^a$	k_{-a} $(s^{-1})^b$	K $(M^{-1})^c$	k_a $(M^{-1}\ s^{-1})^a$	k_{-a} $(M)^b$	K $(M^{-1})^c$	k_a $(M^{-1}\ s^{-1})^a$	k_{-a} $(s^{-1})^b$	K $(M^{-1})^c$
AN	0.65	$\sim 1.2^d$	$\sim 0.55^d$	<0.1			3.7	9.25	0.40
MA	2.0	20	0.10	<0.2			6.0	15	0.40
VA	5.6	1400	0.004	<0.2			8.0	800	0.01
VE	6.0	200	0.03	<0.2			10.0	125	0.08

[a] In $10^5\ M^{-1}\ s^{-1}$. [b] In $10^5\ s^{-1}$. [c] Using a k_{02} value of $3 \times 10^9\ M^{-1}\ s^{-1}$. [d] In the extrapolation procedure, the slope is very small and this value is associated with a lower accuracy. Relatively different values were obtained for the R_3/AN and R_3/VA systems previously investigated in cyclohexane using a flash photolysis system (10 μs flash duration).[12] Because we found no noticeable solvent effect (experiments were carried out in acetonitrile, benzene and cyclohexane), this difference can be likely ascribed to the technique used in ref 12, which has required a rather difficult zero extrapolation procedure due to the time resolution.

TABLE 3: Electronic Properties for the Four Alkenes and the Three Radicals Used[a]

	IP (eV)[b]	EA (eV)[b]	χ (eV)[b]
AN	10.5 (10.9)	0.12 (−0.2)	5.3 (5.4)
MA	9.64 (9.9)	0.09 (−0.5)	4.9 (4.7)
VA	8.91 (9.2)	−0.48 (−1.2)	4.2 (4.0)
VE	8.31 (8.8)	−1.5 (−2.2)	3.4 (3.3)
R_1	8.38	2.98	5.68
R_2	7.98	2.71	5.34
R_3	8.23	2.98	5.61

[a] See text. [b] At UB3LYP/6-31+G* and ZPE corrected. In brackets are the experimental data from ref 1.

Another possibility to investigate large systems with a high-level procedure obviously consists of introducing a simplification of the chemical system. However, in the present case, this option has been ruled out because of the large delocalization of the SOMO in R_1-R_3 that prevents any reduction of the π system. Therefore, it has been decided to moderate the computational cost and to maintain the chemical integrity of the system to reproduce the trends even if the calculated barriers exhibit a higher uncertainty.

(b) Comparison with the Experimental Data. The alkenes were characterized in terms of electron donor/acceptor properties. Calculated adiabatic ionization potentials (IP) and adiabatic electron affinities (EA) are collected in Table 3. The electron deficient or electron-rich character of the different alkenes is represented by their absolute electronegativity (χ) calculated from eq 6:[47,48]

$$\chi = (\mathrm{IP} + \mathrm{EA})/2 \qquad (6)$$

The electron acceptor properties of the four alkenes are expected to increase with the absolute electronegativity in the series VE, VA, MA, and AN. The good agreement between the calculated and the experimental values shows that the computational method is accurate enough to describe the electron donor/acceptor properties of the double bonds. The same procedure was used to obtain the absolute electronegativity (χ_R) of the radicals (Table 3).

The different parameters characterizing the addition process (ΔH_R, δ^{TS}, and E_a) are gathered in Table 4. The trends for the calculated barriers of the addition reaction are found in excellent agreement with those obtained for the measured addition rate constants k_a. For a given radical, the reactivity decreases in the series VE > VA > MA > AN. For a given alkene, the reactivity follows the order $R_3 > R_1 > R_2$ (in the case of R_2, a limit value of $2 \times 10^4\ M^{-1}\ s^{-1}$ has been estimated). The agreement between the experimental and calculated reactivity orders confirms that the selected DFT procedure is usable.[51]

For a deeper analysis, the rate constants for both the addition and fragmentation processes were evaluated from TST calculations (Table 4). Despite a clear underestimation of k_a (between one and 2 orders of magnitude), a fairly good agreement between the calculated and experimental data can be noted (Figure 4) demonstrating the validity of the computational approach used (the discussions on the fragmentation rate constants will be given in the last part of this article). The trends between k_a and E_a are similar (the slopes of the $\log(k_a) = f(E_a)$ plot are -0.04 ± 0.01 for R_1 and R_3): this evidences a weak influence of the pre-exponential factor. Interestingly, the calculated values are found between 1 and 2 orders of magnitude lower than the experimental ones. This should result from the combination of two different effects: (i) the influence of the solvent is not included (indeed, it has been shown that this factor could affect the preexponential factor[1]) (ii) the TST approach does not explicitly treat the low-frequency torsionnal modes that are considered as vibrations. This factor could also affect the calculated values,

TABLE 4: Thermodynamical Data and Transition State Properties for the Radical/Alkene Couples[a]

system	$\Delta H_R{}^b$ (kJ/mol)	$\Delta H_R{}^c$ (kJ/mol)	$\delta^{TS\ b}$	$\delta^{TS\ c}$	$E_a{}^b$ (kJ/mol)	$\log(k_{a,calc})$	$\log(k_{-a,calc})^d$	$\log(k_{-a,calc})^e$
R_1/AN	−15.3	−23.0	−0.012	−0.059	29.5	2.1	5.8	4.0
R_1/MA	−9.6	−16.3	−0.021	−0.082	26.9	2.5	7.2	5.4
R_1/VA	2.8	−4.1	−0.107	−0.198	24.6	2.9	9.7	7.9
R_1/VE	−5.4	−13.1	−0.237	−0.251	13.5	4.0	10.0	8.3
R_2/AN	−6.0	−13.8	0.030	−0.033	29.7	1.9	7.1	5.4
R_2/MA	0.9	−5.9	0.01	−0.055	28.8	2.0	8.3	6.6
R_2/VA	14.3	7.2	−0.06	−0.159	31.5	1.6	10.1	8.3
R_2/VE	6.42	−1.3	−0.186	−0.259	23.3	2.7	10.6	8.9
R_3/AN	−17.3	−26.0	−0.006	−0.059	23.8	3.0	6.5	4.7
R_3/MA	−11.2	−19.0	−0.009	−0.082	23.3	3.2	7.7	5.9
R_3/VA	1.7	−6.5	−0.109	−0.190	15.1	4.5	11.2	9.5
R_3/VE	−6.1	−14.9	−0.207	−0.246	13.1	5.0	9.7	8.0

[a] See text. [b] Single points at the UB3LYP/6-311++G** level on the geometry determined at the 6-31G* level, ZPE corrected at the 6-31G* level. [c] UB3LYP/6-31G* and ZPE corrected at the 6-31G* level. [d] Using calculated ΔH_R values at the 6-311++G** level. [e] Using new ΔH_R values expressed as ΔH_R (calculated at the 6-311++G** level) − 2.4 kcal/mol.

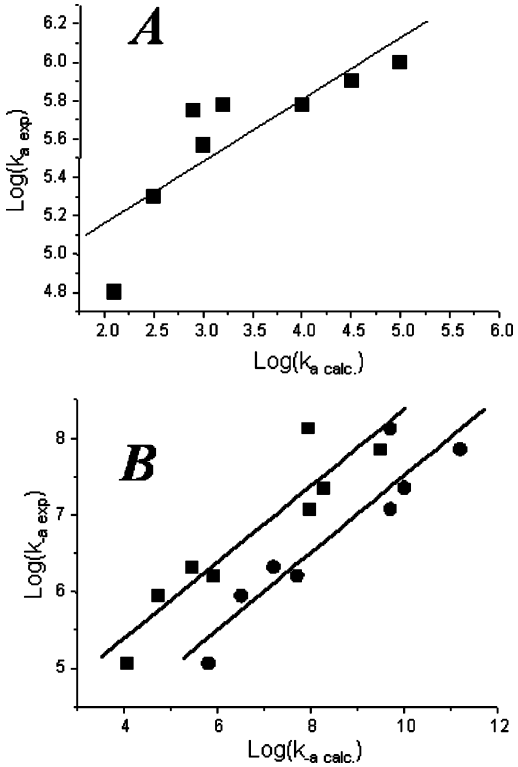

Figure 4. (A) Experimental vs calculated k_a. (B) Experimental vs calculated k_{-a}. Key: (●) $E_{a,-a}$ evaluated from ΔH_R (at the 6-311++G** level); (■) $E_{a,-a}$ evaluated from ΔH_R (at the 6-311++G** level) − 2.4 kcal/mol.

as evidenced recently for the carbon-centered radical addition to the C═S bond.[49,50] The relative reactivity of the different radical/alkene systems can be strongly affected by both the polar and enthalpy effects. The combination of experimental data and quantum mechanical calculations can now allow us to shed some light on their respective influence.

3. Addition Process. (a) Enthalpy Factor. The reaction enthalpies determined with an extended basis set 6-311++G** correlate quite well with those found at the 6-31G* level (Table 4). The reaction exothermicity found at 6-311++G** level is lower by about 7.3 kJ/mol than that found at the 6-31G* level ($\Delta H_{R\ 6-311++G^{**}} = 0.97\ \Delta H_{R\ 6-31G^{*}} + 7.3$ with $R^2 = 0.998$). The same trend was observed for carbon-centered radicals with a difference of 15.6 kJ/mol.[26] In the following discussion, we will consider the results obtained with the extended basis set even if identical trends can be obtained with the 6-31G* level.

A comparison between Tables 3 and 4 and Table 1 shows that the reaction enthalpy does not correlate with the addition rate constants or the barriers. Indeed, the reaction exothermicity decreases in the series AN > MA > VE > VA whereas the reactivity decreases in the opposite order VE > VA > MA > AN. Acrylonitrile, which has the highest exothermicity, exhibits the lowest reactivity. From the state correlation diagram, the barrier is expected to decrease with the reaction exothermicity when going from VA to AN for a given radical. Our results clearly evidence that the enthalpy factor does not govern the reactivity of the systems studied here. This unexpected behavior of MBO-, MBI-, and MBT-derived radicals must be outlined because the reactivity of aryl thiyl radicals was clearly considered as influenced by the reaction exothermicity.[13]

For carbon-centered radicals,[27] the reaction exothermicity decreases in the series AN > MA > VA > VE; i.e., electron withdrawing substituents increase the alkene electronegativity and stabilize the newly formed radical. In contrast, in sulfur-centered radicals, a noticeable inverse order between VA and VE is noted. This result can be clearly ascribed to the important charge transfer observed in the adduct radical, which implies a large spin delocalization not only on the alkene substituent but also on the sulfur atom. The good correlation observed between the alkene electonegativity and the sulfur spin population in the adduct radical evidences this important aspect (Figure 5). As a consequence, the reaction exothermicity is affected by two factors that influence the stability of the product, i.e., the spin delocalization on the sulfur atom (which increases from AN to VE) and the presence of electron withdrawing substituents on the alkene (which increases the effect from VE to AN). The combination of these two antagonist factors explains the unusual change of the reaction exothermicity for sulfur-centered radicals compared to that found for carbon-centered ones.[27]

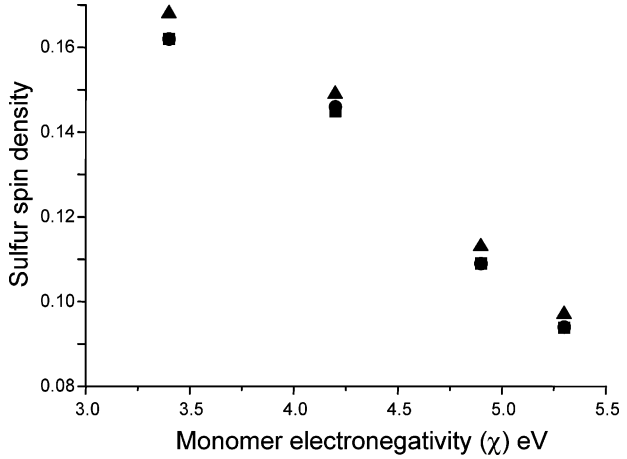

Figure 5. Change of the spin density on the sulfur atom in the adduct radical with the alkene electronegativity: R_1 (■); R_2 (▲); R_3 (●).

(b) Polar Effects. The importance of the polar effects is usually reflected[25−28] by the amount δ^{TS} of the charge transfer in the transition state. Unlike the case of carbon-centered radicals, a noticeable basis set effect on δ^{TS} is observed. The δ^{TS} values determined at the 6-31G* level are systematically higher than those calculated at the 6-311++G** level ($\delta^{TS}_{6-311++G^{**}} = 1.03\ \delta^{TS}_{6-31G^{*}} + 0.068$ with $R^2 = 0.94$).

The sulfur-centered radicals are found to be electrophilic, in line with their very high electronegativity (Table 3), with a neat charge transfer from the alkene to the radical (δ^{TS} is negative). The electrophilic character of these structures toward acrylonitrile is particularly striking. Indeed, acrylonitrile, bearing a strong withdrawing substituent, is usually a very good electron acceptor. However, its electronegativity is lower than those of the R_1 and R_3 radicals and the charge transfer is thus observed from the alkene to these radicals. The neat charge transfer from the alkene to the radical found in the TS structure correlates quite well with the electronegativity of the alkenes: it considerably increases (Figure 6) in the series AN < MA < VA < VE for a given radical and from R_2 to $R_1 \sim R_3$ for a given alkene. This trend corresponds to the experimental change of k_a. These polar effects become very important as exemplified by a δ^{TS} higher than 0.2 for the addition to VE. This value is relatively similar (in absolute unit) to those reported for the addition of nucleophilic aminoalkyl radicals to MA whose reactivity is strongly governed by their charge-transfer properties.[25−26]

Therefore, the polar effect appears as the major factor affecting the R_1-R_3 reactivity. Contrary to previous results reported in the literature for other sulfur radicals,[13] the enthalpy factor must not be considered here as the key parameter for the addition of sulfur radicals to monomers. Radicals having a high electro-

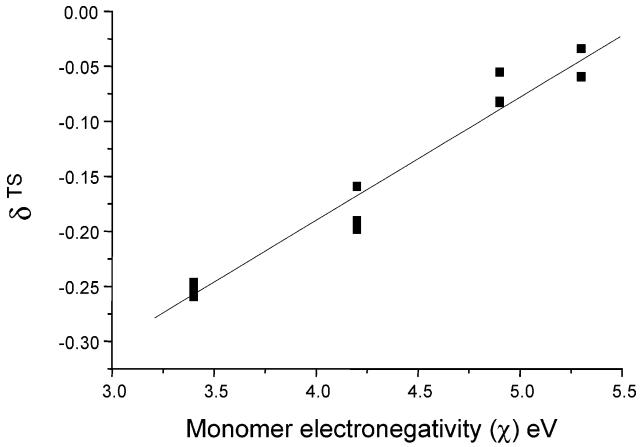

Figure 6. Change of δ^{TS} with the alkene electronegativity for the different radical/alkene couples.

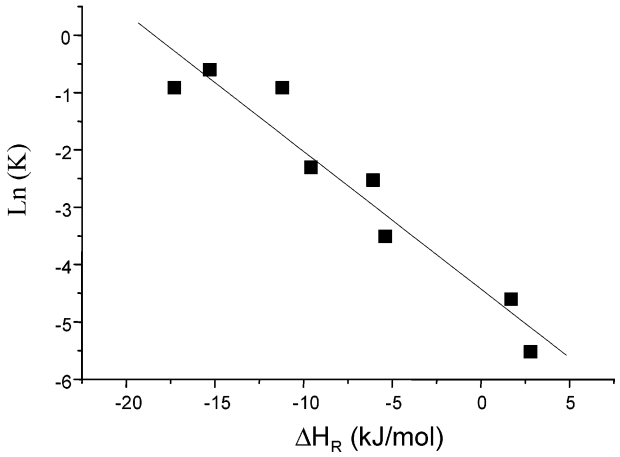

Figure 7. Correlation between the logarithm of the equilibrium constant (experiment) and the reaction enthalpy.

negativity (R_1 and R_3) will exhibit a high charge transfer in the TS structure, thereby decreasing the barrier for the addition process. For R_2, the lower electronegativity decreases the polar effect. The concomitant lowest exothermicity of this structure also explains quite well its lowest reactivity. This result is in full agreement with the calculated k_a (Table 4).

4. Fragmentation Process. The selective radical trapping flash photolysis method[12−15] recalled above is particularly worthwhile for the experimental determination of both the addition and fragmentation rate constants leading to a direct access to the equilibrium constant of the process. For other sulfur-centered radicals, this reversibility has been the subject of many experimental efforts but the factors that govern the reversibility remain unknown.[12−15,33] Here, our experimental parameters (k_a, k_{-a}, K) can be fitted with the reaction enthalpy obtained by quantum mechanical calculations. K decreases with ΔH_R in the series AN > MA > VE > VA (Table 2). Therefore, ΔH_R appears as a key parameter that governs the addition/fragmentation process: $\ln(K)$ is found directly proportional to ΔH_R (Figure 7). A linear fit leads to eq 7.

$$\ln(K) = -0.25\Delta H_R - 4.42 \qquad (R^2 = 0.96) \qquad (7)$$

The associated barrier was evaluated by quantum mechanical calculations (Table 4). Because the TS structures were found to be identical in this study for both the addition and fragmentation processes, the barrier for the back-process ($E_{a,-a}$) is directly related (eq 8) to both the barrier for the addition process ($E_{a,a}$) and the addition reaction enthalpy (ΔH_R).

$$E_{a,-a} = E_{a,a} - \Delta H_R \qquad (8)$$

Assuming that k_a and k_{-a} can be described by a classical Arrhenius equation (eq 9), where A represents the preexponential factor, the equilibrium constant is expressed by eq 10. Taking eq 8 ($-\Delta H_R = E_{a,-a} - E_{a,a}$), it becomes

$$k = A \exp(-E_a/RT) \qquad (9)$$

$$\ln(K) = \ln(A_a/A_{-a}) - \Delta H_R/RT \qquad (10)$$

Identifying eqs 7 and 10, the experimental slope (−0.25) appears rather close to the theoretical value $-1/RT$ (−0.4). However, the preexponential factor for the fragmentation process is found about 80 times higher than that corresponding to the addition reaction ($\ln(A_a/A_{-a}) = -4.42$). This approach, which used the calculated exothermicity, leads to physically unrealistic frequency factors, as it can be expected that the frequency factors for unimolecular (fragmentation) or bimolecular (addition) only differ by about 5 orders of magnitude. This difference is obviously related to the procedure used for the ΔH_R calculations, which are affected by the basis set (see above).

From the fragmentation barriers calculated through eq 8 and using ΔH_R at the 6-311++G** level, the $k_{-a,calc}$ values are found about 2 orders of magnitude larger than the experimental ones (Table 4): this means that the calculated reaction exothermicity (and therefore the barrier) is underestimated. Increasing this exothermicity by a selected constant of 2.4 kcal/mol leads to fragmentation rate constants in good agreement with the experimental data (Table 4 and Figure 4). Such a modification of ΔH_R leads likewise to a realistic ratio of the frequency factors ($\sim 10^4$). These results evidence that an accurate determination of ΔH_R is required for a quantitative study of the fragmentation process. Nevertheless, this change of ΔH_R with the basis set remains reasonable for the calculation of an energetic parameter, as already stated.[30] Moreover, independent of this correction of the exothermicity, good linear relationships are noted for k_{-a} between the calculated and experimental data (the $k_{-a} = f(\Delta H_R)$ curves are obviously parallel when shifting ΔH_R with a selected constant), thereby giving confidence to the present MO calculations to reproduce the observed trend (Figure 4).

Figure 8 shows the specific behavior of k_{-a} and k_a. The $\log(k_{-a})$ values are clearly dependent on the reaction enthalpy: k_{-a} increases when the reaction exothermicity for the addition decreases. The addition reaction (k_a) is mainly affected by the polar effects (weak or almost no dependence between k_a and

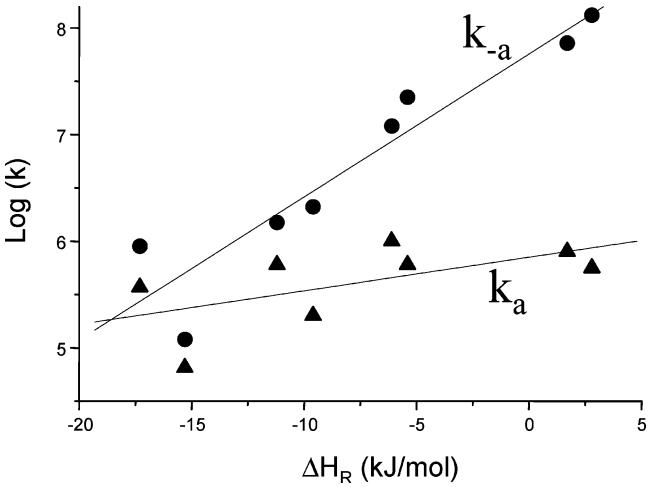

Figure 8. Changes of the calculated addition and fragmentation rate constants with the reaction enthalpy.

ΔH_R). This strong influence of ΔH_R on k_{-a} is in excellent agreement with eq 8: despite the polar effects noted for $E_{a,a}$, the enthalpy term remains preponderant, leading to an apparent k_{-a} vs ΔH_R relationship.

Conclusion

The radical addition reaction of three particular sulfur-centered radicals to double bonds has been investigated both by experiment and by molecular orbital calculations. In the present case, the polar effects appeared as the key factor governing the addition reaction and play a dramatic role; i.e., the R/alkene studied systems exhibiting the highest addition reaction exothermicity are characterized by the lowest reactivity. Alternatively, the back-fragmentation reaction is governed by enthalpy effects: this point has never been mentioned before. A general investigation of the reactivity of very different sulfur-centered radicals certainly remains a fascinating task because a large panel of situations could be expected through a careful selection of mercaptans and double bond compounds. Forthcoming papers will illustrate this aspect as well as the particular behavior of typical sulfur-centered radicals as photoinitiating species in radical polymerization reactions.

Acknowledgment. We thank the CINES (Centre Informatique National de l'Enseignement Supérieur) for the generous allocation of time on the IBMSPsupercomputer.

Supporting Information Available: Complete geometries as coordinates (Gaussian98-03). This material is available free of charge via the Internet at http://pubs.acs.org.

References and Notes

(1) Fischer, H.; Radom, L. *Angew. Chem., Int. Ed.* **2001**, *40*, 1340.

(2) (a) Tedder, J. M. *Angew. Chem., Int. Ed.* **1982**, *21*, 401. (b) Minisci, F. *Free Radicals in Biology and* Environment, Kluwer Academic Publishers: 1997.

(3) Wu, J. Q.; Beranek, I.; Fischer, H. *Helv. Chim. Acta* **1995**, *78*, 194.

(4) Heberger, K.; Lopata, A. *J. Org. Chem.* **1998**, *63*, 8646.

(5) Shaik, S. S.; Shurki, A. *Angew. Chem., Int. Ed.* **1999**, *38*, 586.

(6) Shaik, S. S.; Canadell, E. *J. Am. Chem. Soc.* **1990**, *112*, 1446.

(7) Wong, M. W.; Pross, A.; Radom, L. *J. Am. Chem. Soc.* **1994**, *116*, 6284.

(8) Wong, M. W.; Pross, A.; Radom, L. *J. Am. Chem. Soc.* **1994**, *116*, 11938.

(9) Avila, D. V.; Ingold, K. U.; Lusztyk, J.; Dolbier, W. R.; Pan, H. Q. *J. Am. Chem. Soc.* **1993**, *115*, 1577.

(10) Weber, M.; Khudyakov, I.; Turro, N. J. *J. Phys. Chem. A.* **2002**, *106*, 1938.

(11) (a) Fouassier, J. P. *Photoinitiation Photopolymerization and Photocuring*, Hanser Publishers: Munich, New York, 1995. (b) Lalevée, J.; Allonas, X.; Fouassier, J. P. *J. Am. Chem. Soc.* **2002**, *124*, 9613. (c) Allonas, X.; Lalevée, J.; Fouassier, J. P. in *Photoinitiated Polymerization*, Chapter 12, ACS Symposium Series, 2003, Ed. K. D. Belfield, J. Crivello.

(12) Ito, O.; Nogami, K.; Matsuda, M. *J. Phys. Chem.* **1981**, *85*, 1365.

(13) Ito, O.; Matsuda, M. *Prog. Polym. Sci.* **1992**, *17*, 827.

(14) (a) Alam, M. M.; Konami, H.; Watanabe, A.; Ito, O. *J. Chem. Soc., Perkin Trans. 2* **1995**, 263. (b) Alam, M. M.; Watanabe, A.; Ito, O. *J. Org. Chem.* **1995**, *60*, 3440. (c) Yoshikawa, Y.; Watanabe, A.; Ito, O. *J. Photochem. Photobio. A: Chem.* **1995**, *89*, 209. (d) Ito, O.; Tamura, S.; Matsuda, M.; Kenkichi, M. *J. Polym. Sci: Part A: Polym. Chem.* **1987**, *26*, 1429.

(15) (a) Ito, O.; Matsuda, M. *J. Am. Chem. Soc.* **1979**, *101*, 1815. (b) Ito, O.; Matsuda, M. *J. Am. Chem. Soc.* **1979**, *101*, 5732. (c) Ito, O.; Matsuda, M. *J. Am. Chem. Soc.* **1981**, *103*, 5871. (d) Ito, O.; Matsuda, M. *J. Am. Chem. Soc.* **1982**, *104*, 568. (e) Ito, O.; Matsuda, M. *J. Am. Chem. Soc.* **1982**, *104*, 1701.

(16) Beare, K. D.; Coote, M. L. *J. Phys. Chem. A.* **2004**, *108*, 7211.

(17) Beckwith, A. L. J.; Poole, J. S. *J. Am. Chem. Soc.* **2002**, *124*, 9489.

(18) Zytowski, T.; Knuehl, B.; Fischer, H. *Helv. Chim. Acta* **2000**, *83*, 658.

(19) Heberger, K.; Lopata, A. *J. Chem. Soc. Perkin Trans. 2* **1995**. 91.

(20) Gomez-Balderas, R.; Coote, M. L.; Henry, D. J.; Radom, L. *J. Phys. Chem. A.* **2004**, *108*, 2874.

(21) Zytowski, T.; Fischer, H. *J. Am. Chem. Soc.* **1996**, *118*, 437.

(22) Batchelor, S. N.; Fischer, H. *J. Phys. Chem.* **1996**, *100*, 9794.

(23) Walbiner, M.; Fischer, H. *J. Phys. Chem.* **1993**, *97*, 4880.

(24) Martschke, R.; Farley, R. D.; Fischer, H. *Helv. Chim. Acta* **1997**, *80*, 1363.

(25) Lalevée, J.; Allonas, X.; Fouassier, J. P. *J. Am. Chem. Soc.* **2003**, *125*, 9377.

(26) Lalevée, J.; Allonas, X.; Fouassier, J. P. *J. Phys. Chem. A.* **2004**, *108*, 4326.

(27) Lalevée, J.; Allonas, X.; Fouassier, J. P. *J. Org. Chem.* **2005**, *70*, 814.

(28) Lalevée, J.; Allonas, X.; Fouassier, J. P. *Macromolecules* **2005**, *38*, 4521.

(29) Morlet-Savary, F.; Ley, C.; Jacques, P.; Fouassier, J. P. *J. Phys. Chem. A.* **2001**, *105*, 11026.

(30) (a) Frisch, M. J.; Trucks, G. W.; Schlegel, H. B.; Scuseria, G. E.; Robb, M. A.; Cheeseman, J. R.; Zakrzewski, V. G.; Montgomery, J. A. Jr.; Stratmann, R. E.; Burant, J. C.; Dapprich, S.; Millam, J. M.; Daniels, A. D.; Kudin, K. N.; Strain, M. C.; Farkas, O.; Tomasi, J.; Barone, V.; Cossi, M.; Cammi, R.; Mennucci, B.; Pomelli, C.; Adamo, C.; Clifford, S.; Ochterski, J.; Petersson, G. A.; Ayala, P. Y.; Cui, Q.; Morokuma, K.; Salvador, P.; Dannenberg, J. J.; Malick, D. K.; Rabuck, A. D.; Raghavachari, K.; Foresman, J. B.; Cioslowski, J.; Ortiz, J. V.; Baboul, A. G.; Stefanov, B. B.; Liu, G.; Liashenko, A.; Piskorz, P.; Komaromi, I.; Gomperts, R.; Martin, R. L.; Fox, D. J.; Keith, T.; Al-Laham, M. A.; Peng, C. Y.; Nanayakkara, A.; Challacombe, M.; Gill, P. M. W.; Johnson, B.; Chen, W.; Wong, M. W.; Andres, J. L.; Gonzalez, C.; Head-Gordon, M.; Replogle, E. S.; Pople, J. A. *Gaussian 98*, revision A.11; Gaussian, Inc.: Pittsburgh, PA, 2001. (b) Foresman, J. B.; Frisch, A. In *Exploring Chemistry with Electronic Structure Methods*, 2nd ed.; Gaussian Inc.: Pittsburgh, PA, 1996.

(31) (a) Arnaud, R.; Subra, R.; Barone, V.; Lelj, F.; Olivella, S.; Solé, A.; Russo, N. *J. Chem. Soc., Perkin Trans II* **1986**, 1517. (b) Arnaud, R.; Bugaud, N.; Vetere, V.; Barone, V. *J. Am. Chem. Soc.* **1998**, *120*, 5733.

(32) (a) Pacey, P. D. *J. Chem. Educ.* **1981**, *58*, 612. (b) Steinfeld, J. I.; Francisco, J. S.; Hase, W. L. *Chemical Kinetics and Dynamics*, 2nd ed.; Prentice Hall: Englewood Cliffs, NJ, 1998.

(33) (a) Alfassi Z. B. *The Chemistry of Free Radicals: S−Centered Radicals*; John Wiley & Sons: New York, 1999. (b) Denisov, E. T.; Denisova, T. G.; Pokidova, T. S. *Handbook of Free Radical Initiators*; John Wiley & Sons: New York, 2003. (c) Lochschmidt, A.; Eilers-Konig, N.; Heineking, N.; Ernsting, N. P. *J. Phys. Chem. A* **1999**, *103*, 1776. (d) Ernsting, N. P. *Chem. Phys. Lett.* **1990**, *166*, 221.

(34) Denisov, E. T. *Kinet. Catal.* **2001**, *42*, 23.

(35) Pappas, S. P. *Radiation Curing Science and Technology*; Plenum Press: New York, 1992.

(36) Scaiano, J. C. *J. Phys. Chem.* **1981**, *85*, 2851.

(37) Tozer, D. J.; Amos, R. D.; Handy, N. C.; Roos, B. O.; Serrano-Andres, L. *Mol. Phys.* **1999**, *97*, 859.

(38) Lalevée, J.; Allonas, X.; Fouassier, J. P. *Chem. Phys. Lett* **2005**, *415*, 287.

(39) Finn, M.; Friedline, R.; Suleman, N.; Wohl, C. J.; Tanko, J. M. *J. Am. Chem. Soc.* **2004**, *126*, 7578.

(40) Borges dos Santos, R. M.; Muralha, V. S. F.; Correia, C. F.; Guedes, R. C.; Costa Cabral, B. J.; Martinho Simoes, J. A. *J. Phys. Chem. A* **2002**, *106*, 9883.

(41) Izgorodina, E. I.; Coote, M. L.; Radom, L. *J. Phys. Chem. A* **2005**, *109*, 7558.

(42) Izgorodina, E. I.; Coote, M. L. *J. Phys. Chem. A* **2006**, *110*, 2486.

(43) Henry, D. J.; Parkinson, C. J.; Radom, L. *J. Phys. Chem. A* **2002**, *106*, 7927.

(44) Coote, M. L.; Wood, G. P. F.; Radom, L. *J. Phys. Chem. A.* **2002**, *106*, 12124.

(45) Coote, M. L.; Easton, C. J.; Zard, S. Z. *J. Org. Chem.* **2006**, *71*, 4996.

(46) Coote, M. L.; Izgorodina, E. I.; Cavigliasso, G. E.; Roth, M.; Busch, M.; Barner-Kowollik, C. *Macromolecules* **2006**, *39*, 4585.

(47) Parr, R. G.; Pearson, R. G. *J. Am. Chem. Soc.* **1983**, *105*, 7512.

(48) Pearson. R. G. *J. Am. Chem. Soc.* **1985**, *107*, 6801.

(49) Coote, M. L. *Macromolecules* **2004**, *37*, 5023.

(50) Henry, D. J.; Coote, M. L.; Gomez-Balderas, R.; Radom, L. *J. Am. Chem. Soc.* **2004**, *126*; 1732.

(51) As suggested by a reviewer, for the DFT procedure selected, the errors in the trends are likely smaller than the absolute values. Despite the larger errors of the DFT procedure (compared to the G2-MP2-RAD procedure, for example), this treatment appears for the present work as quite acceptable to understand the factors governing the studied radicals' reactivities. For a complete analysis, a more refined treatment must be adapted.